Abstract

Mitral valve regurgitation is a heart valve disorder resulting in the backflow of blood. This leads to complications that necessitate an annuloplasty surgery, where the mitral valve is tightened with an annuloplasty ring. The conventional procedure to insert the ring into the heart involves a 25-30 cm skin incision and median sternotomy, which is surgically taxing on the patient. To alleviate this issue, in this project, novel rings were constructed using the shape-memory alloy Nitinol and shape memory polymer MMA-PEGDMA, both of which are biocompatible. These materials are thermosensitive, and will revert to their trained shape when heated, even when initially deformed. Hence, rings made from such materials can be compressed, and inserted into the heart through a smaller incision. Once inside the heart, the core body temperature causes the ring to return to its intended shape. In addition, MMA-PEGDMA is biodegradable, making the procedure suitable for growing children. Subsequently, the effectiveness of the rings was tested, based on four key metrics: reduction in incision size, time taken for shape recovery, the reduction of regurgitation, and flexibility inside the heart. The results show that both materials are exceptional candidates for annuloplasty rings, as both rings successfully transitioned between shapes and decreased regurgitation significantly. The success of this experiment is a major breakthrough for minimally invasive surgical procedures, allowing minimally invasive techniques to be applied on annuloplasty surgeries.

Report

1 Introduction

Mitral valve regurgitation (MR) is caused by the retrograde flow of blood from the left ventricle into the left atrium through the mitral valve [1], causing a systolic murmur, best heard at the left fifth midclavicular line with possible radiation to the left axilla [2]. MR is the most common valvular heart disease [3], of which primary MR is a disease of the mitral valve apparatus, whereas secondary MR is a disease of the left ventricle [4]. Primary MR arise when the normal interactions between the mitral valve leaflets, annulus, papillary muscles and chordae tendinae are disrupted [5].

The first successful surgical approach to MR was first reported in 1951, through a left thoracotomy, after which the mitral annulus was narrowed by external constriction of the base of the heart [6]. Since then, surgical repair has become the reference standard treatment in primary MR [7], which commonly entail mitral valve repair or replacement [5]. In the annuloplasty procedure, an annuloplasty ring is used to tighten or reinforce the annulus of the valve [8], to ensure the closure of the mitral valve leaflets.

The mitral valve can be accessed via the left atrium or ventricle [9], which require skin incisions. Various surgical approaches have been used, including sternotomy [10, 11], thoracotomy [12], or percutaneous access [13]. Of these, median sternotomy is the primary surgical approach considered [17], due to its reliability and speed [6]. However, this typically requires a 25 to 30 centimeter skin incision [15] and splitting of the sternum. This is highly taxing on the patient, and can lead to scarring [16] or surgical fatigue.

Consequently, minimally invasive surgery procedures are preferred, where smaller incisions are made. However, the conventional silicone "Physio" annuloplasty rings are rigid, and often parachuted down filament wires into the annulus [17]. As such, the size of the incision needs to be of a sufficient size to allow the horizontal insertion of the rigid ring. In

addition, though percutaneous access provides a minimally invasive possibility, this requires a trade-off with effectiveness and ease of application [15], due to the plasticity of the device.

The need for an effective minimally-invasive alternative to the conventional annuloplasty procedures is apparent. This alternative procedure necessitates a ring which is easily deformed initially, but becomes rigid once affixed to the annulus. In this project, such an annuloplasty ring is proposed, and its effectiveness is investigated via various metrics.

2 Objectives

The construction of an annuloplasty ring that is able to transition between plastic and rigid states is possible with the use of *thermosensitive* shape-memory materials. These materials can be trained to "remember" a specific shape, and will always return to this trained shape when they are heated past a critical transition temperature. At the high temperature, the material is rigid, yet below this transition temperature, the material is flexible and can be bent into any other shape.

Via this unique Shape-Memory Effect, the annuloplasty ring can be compressed and inserted into the heart as a thin rod (Fig. 1, left). Once in the heart, the body's higher core temperature will cause the rod to return to a rigid ring shape (Fig. 1, right), which can then be sutured onto the annulus.

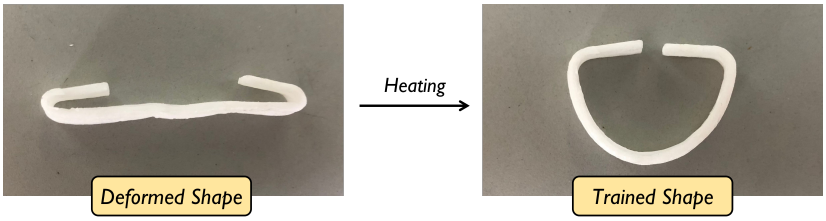

Figure 1: Transformation from deformed to trained shape upon heating

The objective of this research is to investigate the ability of the materials to reduce incision size, the recovery time taken, the efficacy of these rings in reducing backflow, and the flexural rigidity of the rings within the heart.

This novel research place focus on two shape memory materials: the biocompatible Nitinol[1] shape-memory alloy and the biocompatible, biodegradable MMA-PEGDMA[2] shape-memory copolymer. The biodegradability of MMA-PEGDMA allows the ring to be more suited for growing hearts. As the ring gradually degrades, cardiac cells can grow around it, reinforcing the shape of the annulus naturally [19]. Given the higher prevalence of mitral valve-related genetic diseases [20] in adolescents [21], these rings will reduce reliance on the ring as the heart develops fully, allowing young patients to have a higher rate of recovery.

3 Mechanisms

First, the mechanisms allowing for the shape memory effect exhibited by both rings, as well as the biodegradability of the MMA-PEGDMA ring is discussed.

3.1 Shape Memory Effect

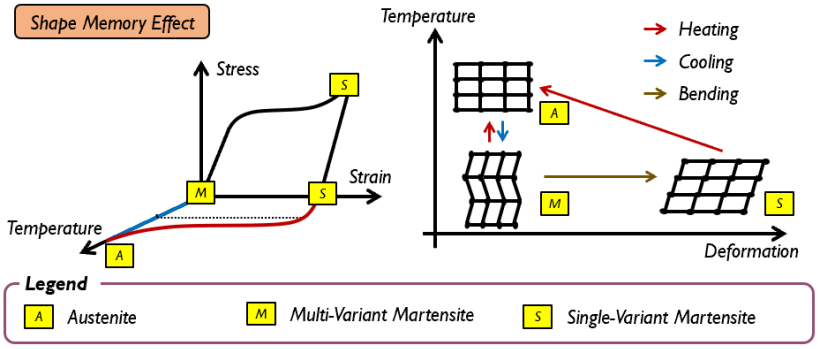

Figure 2: Shape Memory Effect of Nitinol

In Shape-Memory Alloys, monoclinic multi-variant martensite undergoes detwinning instead of irreversible deformation, transforming into single-variant martensite with the application of an external stress. The shape-memory effect refers to the transformation between the martensitic and austenitic phases. When the temperature is raised beyond the austenite start temperature, both single and multi-variant martensitic fractions assume the interpenetrating simple cubic structure austenite, which reverts to multi-variant martensite as the

[1]Nitinol: an alloy of Nickel and Titanium, discovered at the Naval Ordnance Laboratory
[2]MMA-PEGDMA: Methyl Methacrylate-Polyethylene Glycol Dimethacrylate

temperature is lowered. Since austenite and multi-variant martensite have the same macroscopic structure, the original shape of the material is restored.

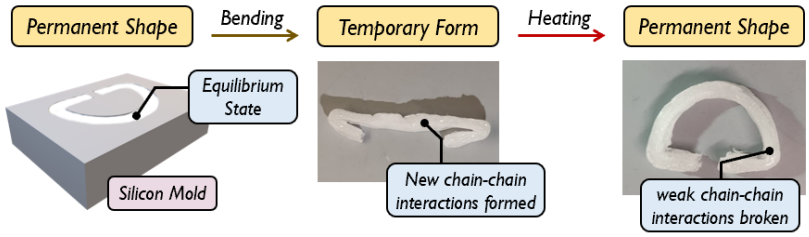

Figure 3: Shape Memory Effect of MMA-PEGDMA

The MMA-PEGDMA copolymer displays the shape-memory effect via a different mechanism. The copolymer is made via the silicon mould to have a stored permanent shape in the form of the annuloplasty ring. As it sets in the mould, the polymer forms in a way that minimizes strain and is at its equilibrated state. When deformed, it forms new chain-chain interactions that keep it in its temporary form. However, upon heating, these weak chain-chain interactions are broken, and it returns to their original permanent shape.

3.2 Biodegradability

The biodegradibility of MMA-PEGDMA is attributed to its hydrolysable ester backbone (Figure 4). A unit of MMA-PEGDMA is depicted on the left. After being sutured onto the annulus, the backbone of MMA-PEGDMA gradually hydrolyses over time [25], forming nontoxic byproducts PEG[3] and PMMA[4].

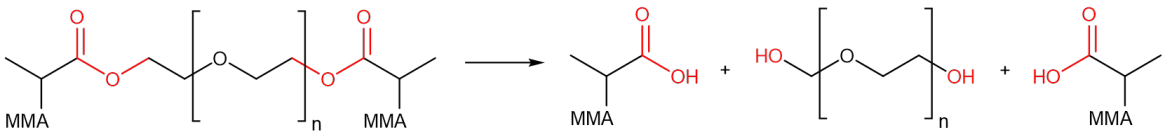

Figure 4: Hydrolysis of MMA-PEGDMA

[3]PEG: Polyethylene Glycol
[4]PMMA: Polymethyl Methacrylate

4 Methodology

4.1 Making the Annuloplasty Rings

To make the Nitinol ring, a sizer is used to measure the annulus and construct the D-shaped annulus ring with the measured dimensions. To reduce mechanical stress on the atrial walls, the ring is wrapped in bovine myocardium. This also serves to further increase the compatibility of the ring, reducing chances of body rejection after surgery [23]. Rings of thicknesses 0.25mm, 0.50mm and 1.00mm were made.

To create the MMA-PEGDMA copolymer rings, an elastic mold is first made by adding silicon rubber mix to a 3D-printed negative mold. We mix PMMA[5], PEGDMA[6], and DMPA initiator[7] in a 6:3:2 ratio, using acetone as the solvent. The copolymer, which is precipitated out when deionised water is added, is loaded into the silicon mould where it sets and is trained in the ring shape. A total of 6 rings were made, each of different thickness: 1.00mm, 2.00mm, 3.00mm, 4.00mm, 5.00mm and 6.00mm.

4.2 Testing the Annuloplasty Rings

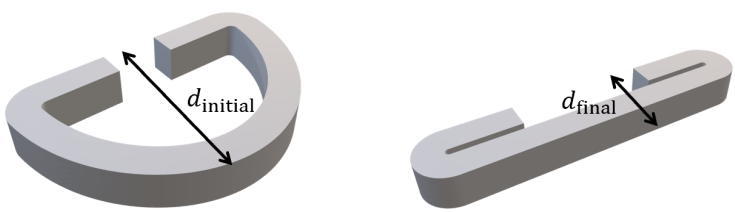

Figure 5: Method of determining the reduction in incision size

The effectiveness of the rings depends on four key metrics: compressibility, shape-memory effect, the reduction of regurgitation, and flexibility. The compressibility is given by the **reduction in incision size**, when the ring is compressed to d_{final}, the minimum cross-section where it can still undergo shape recovery (Equation 4.1).

[5]PMMA: Poly(Methyl Methacrylate)
[6]PEGDMA: Polyethylene Glycol Dimethacrylate
[7]DMPA: Dimethylol Propionic Acid, a radical initiator catalysing alkene polymerisation of PMMA and PEGDMA

$$\%_{\text{min}} = \frac{\text{change in cross-sectional size}}{\text{initial width of ring}} = \frac{d_{\text{initial}} - d_{\text{final}}}{d_{\text{initial}}} \tag{4.1}$$

The **recovery time** is also measured, which is the time taken for the wire to transform from maximum deformation back to the original trained shape. This gives an indication of the time that can be allocated for the deformed ring to be inserted into the heart and how suitable each size is to be used during surgery.

Next, the **efficacy of the ring** in reducing mitral valve regurgitation is tested by measuring the static backflow before and after ring insertion. The static backflow is defined as height of water above the annulus, and is related to the backflow velocity by $v_{\text{backflow}} = \sqrt{2gh}$. The mitral valve is induced to leak and water is pumped through the aorta into the ventricle to artificially mimic the backflow of blood at a volumetric flow rate of 40.5cm^3/s.

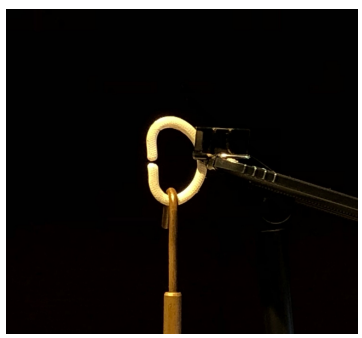

Figure 6: Setup for elastic modulus characterisation (Physio ring is shown)

Finally, the **flexural rigidity** of the Nitinol, MMA-PEGDMA and the commonly used Physio rings were characterised and compared. Weights were hung from the annuloplasty rings (Fig.6), extending it, and the resulting radius of curvature R formed is obtained using Tracker[8], by fitting the curved section to a circle. The strain ε and stress σ are given by equation (2.2), where t is the thickness of the ring and R is the outer radius of curvature.

$$\varepsilon = \frac{t}{2}\left(\frac{1}{R_{\text{initial}}} - \frac{1}{R}\right) \qquad \sigma = \frac{4mg}{\pi t^2}\left(\frac{1}{2(R-t)^2} - \frac{1}{2R^2}\right) \tag{4.2}$$

[8]Tracker: a computational pixel-counting software

The material-specific elastic modulus E is obtained from the gradient of the stress-strain plot, allowing the determination the geometry-specific flexural rigidity D as a function of the ring thickness via $D = EI$, where I is the moment of inertia[9].

5 Results and Discussion

5.1 Reduction in Incision Size

For both the Nitinol and MMA-PEGDMA rings, the high % reduction in incision size allows the ring to be inserted through the ribs in a minimally invasive manner.

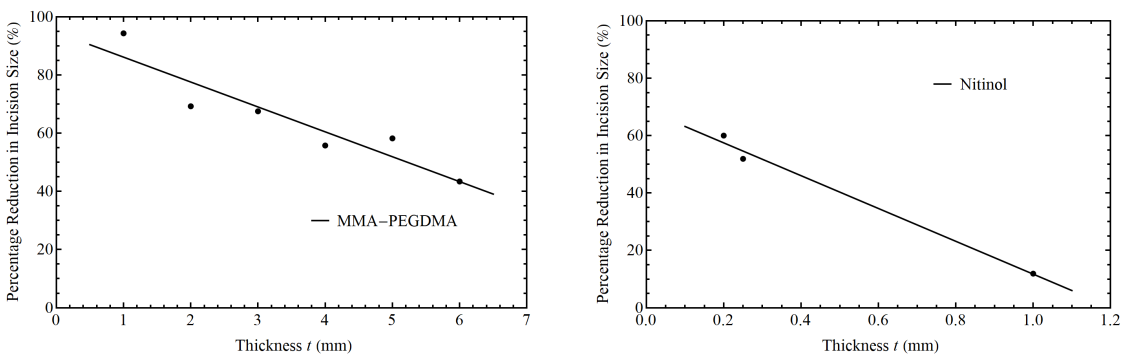

Figure 7: % Reduction in incision size for MMA-PEGDMA (left), Nitinol (right) rings

5.2 Recovery Time

From Table 1 and 2, the results show that in 60°C water, the recovery time varies proportionally with the wire thickness and can therefore be controlled and tailored to different surgical procedures by altering the wire thickness.

[9]The expression for moment of inertia is derived in the Appendix

Wire Thickness (mm)	Initial Shape	Final Shape	Time Taken (s)
0.25			0.11
0.50			3.99
1.00			7.99

Table 1: Recovery time for Nitinol rings

Wire Thickness (mm)	Initial Shape	Final Shape	Time Taken (s)
1.00			7.30
2.00	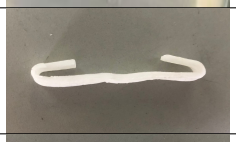	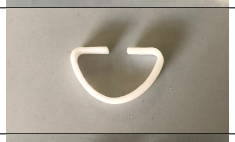	11.98
3.00	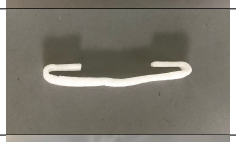	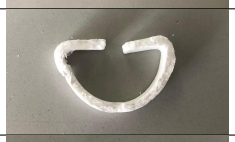	14.78
4.00			18.26
5.00			26.31
6.00			28.32

Table 2: Recovery time for MMA-PEGDMA rings

5.3 Efficacy of Rings

The static regurgitation of the Nitinol and MMA-PEGDMA annuloplasty rings were compared against that of the Physio ring. The swine heart used had an inner trigone distance

of 3.7cm and an anterior-posterior distance of 2.1cm. In comparison, Physio rings reduce regurgitation volume by 44% [24]. From the results, it is evident that the Nitinol and MMA-PEGDMA annuloplasty rings were comparably effective as the Physio ring in reducing mitral valve regurgitation.

Ring	Initial Static Regurgitation	Final Static Regurgitation	Initial Flow Rate	Final Flow Rate	% Reduct.
Nitinol	13 mm	4.3 mm	0.51 m/s	0.29 m/s	43%
MMA-PEGDMA	15 mm	4.0 mm	0.54 m/s	0.28 m/s	48%

Table 3: Percentage reduction of mitral valve regurgitation for both rings

5.4 Flexural Rigidity

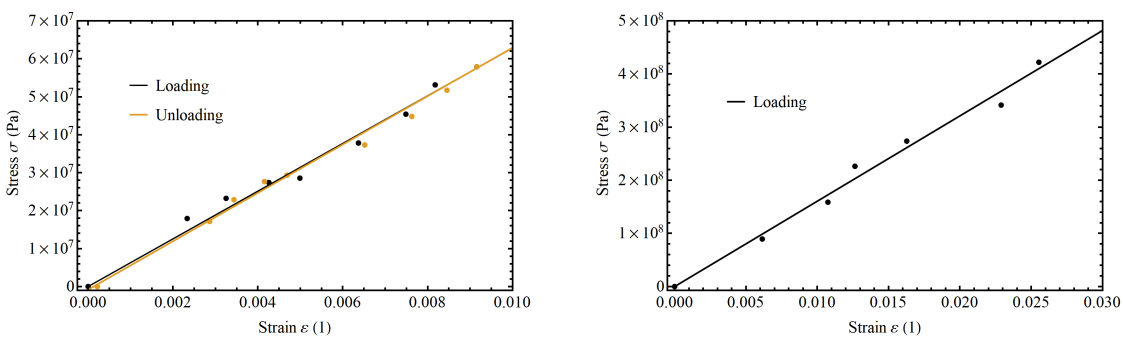

Figure 8: Stress-strain characterisation curve of MMA-PEDGMA (left), Physio ring (right)

The elastic modulus of the MMA-PEGDMA and Physio rings was first characterised via the gradient of the stress-strain curve (Fig. 8). From the characterisation,

$$E_{\text{MMA}} = 6.285 \text{ GPa} \qquad E_{\text{Physio}} = 16.06 \text{ GPa} \tag{5.1}$$

in comparison with $E_{\text{Nitinol}} = 83$ GPa[10]. Next, the flexibility of the rings were compared, and it was observed that both the Nitinol and MMA-PEGDMA rings allow a wider range of flexural rigidity, and have a lower mean flexural rigidity lower than the Physio ring, which gives the heart more flexibility, which is desired.

[10] https://matthey.com/en/products-and-services/medical-components/resource-library/nitinol-technical-properties

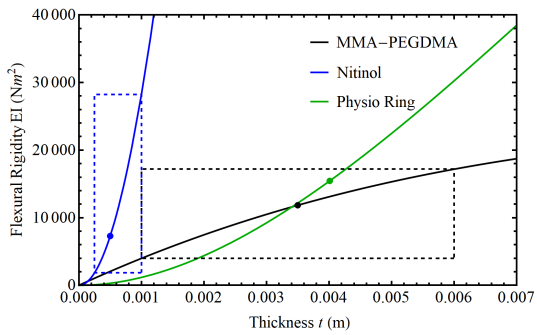

Figure 9: Flexural rigidity of rings: box indicate range of thickness investigated for each material, dot represents mean thickness

6 Conclusion

The success of the experiment is a major breakthrough for minimally invasive surgical procedures. By applying these novel rings to current minimally invasive surgical techniques, these rings can be deformed into a rod shape to be inserted through the ribs using a smaller incision. This eliminates the necessity of the surgically taxing median sternomy from the procedure, reducing the possibility of complications involving heavy scarring.

Besides having important applications in minimally invasive procedures, the biodegradability of the MMA-PEGDMA ring provides room for growth, encouraging proliferation of cardiac cells and decreasing reliance on the ring in the long term. Future work would include tests on live animals, and the monitoring the hearts in the long term.

In conclusion, Nitinol and MMA-PEGDMA annuloplasty rings were successfully made for minimally invasive surgical procedures. The rings demonstrated their ability to undergo shape recovery, and reduce mitral valve regurgitation. The higher flexibility of the shape memory rings also provides the heart with a larger degree of freedom to contract, further emphasizing the efficacy of the rings.

References

[1] Douedi, S., Douedi, H. (2020). Mitral Regurgitation.

[2] Thomas, S. L., Heaton, J., Makaryus, A. N. (2021). Physiology, cardiovascular murmurs. In StatPearls [Internet]. StatPearls Publishing.

[3] Hollenberg, S. M. (2017). Valvular Heart Disease in Adults: Etiologies, Classification, and Diagnosis. FP essentials, 457, 11-16.

[4] El Sabbagh, A., Reddy, Y. N., Nishimura, R. A. (2018). Mitral valve regurgitation in the contemporary era: insights into diagnosis, management, and future directions. JACC: Cardiovascular Imaging, 11(4), 628-643.

[5] Apostolidou, E., Maslow, A. D., Poppas, A. (2017). Primary mitral valve regurgitation: Update and review. Global cardiology science practice, 2017(1).

[6] Bailey, C. P., O'NEILL, T. J., Glover, R. P., Jamison, W. L., Ramirez, H. P. R. (1951). Surgical repair of mitral insufficiency:(a preliminary report). Diseases of the Chest, 19(2), 125-137.

[7] De Bonis, M., Al-Attar, N., Antunes, M., Borger, M., Casselman, F., Falk, V., ... Prendergast, B. (2016). Surgical and interventional management of mitral valve regurgitation: a position statement from the European Society of Cardiology Working Groups on Cardiovascular Surgery and Valvular Heart Disease. European heart journal, 37(2), 133-139.

[8] Borregaard, B. (2022). Surgical Treatment for Patients with Valvular Heart Disease. In Valvular Heart Disease (pp. 151-165). Springer, Cham.

[9] Shone, J. D., Sellers, R. D., Anderson, R. C., Adams Jr, P., Lillehei, C. W., Edwards, J. E. (1963). The developmental complex of "parachute mitral valve," supravalvular ring of left atrium, subaortic stenosis, and coarctation of aorta. The American journal of cardiology, 11(6), 714-725.

[10] Sundermann, S. H., Sromicki, J., Biefer, H. R. C., Seifert, B., Holubec, T., Falk, V., Jacobs, S. (2014). Mitral valve surgery: right lateral minithoracotomy or sternotomy? A

systematic review and meta-analysis. The Journal of thoracic and cardiovascular surgery, 148(5), 1989-1995.

[11] Iribarne, A., Russo, M. J., Easterwood, R., Hong, K. N., Yang, J., Cheema, F. H., ... Argenziano, M. (2010). Minimally invasive versus sternotomy approach for mitral valve surgery: a propensity analysis. The Annals of thoracic surgery, 90(5), 1471-1478.

[12] Al Otaibi, A., Gupta, S., Belley-Cote, E. P., Alsagheir, A., Spence, J., Parry, D., Whitlock, R. P. (2016). Mini-thoracotomy vs. conventional sternotomy mitral valve surgery: a systematic review and meta-analysis. The Journal of Cardiovascular Surgery, 58(3), 489-496.

[13] Shah, M., Jorde, U. P. (2019). Percutaneous mitral valve interventions (repair): current indications and future perspectives. Frontiers in cardiovascular medicine, 6, 88.

[14] Glauber, M., Miceli, A. (2015). State of the art for approaching the mitral valve: sternotomy, minimally invasive or total endoscopic robotic?. European Journal of Cardio-Thoracic Surgery, 48(5), 639-641.

[15] Glower, D. D., Landolfo, K. P., Clements, F., Debruijn, N. P., Stafford-Smith, M., Smith, P. K., Duhaylongsod, F. (1998). Mitral valve operation via port access versus median sternotomy. European journal of cardio-thoracic surgery, 14(Supplement_1), S143-S147.

[16] Jina, H., Simcock, J. (2011). Median sternotomy scar assessment. NZ Med J, 124(1346), 57-62.

[17] Glauber, M., Ferrarini, M., Miceli, A. (2015). Minimally invasive mitral valve repair using a semi-rigid annuloplasty ring with a new chordal sizing system: the Memo3D ReChord. Annals of cardiothoracic surgery, 4(3), 298.

[18] Cosgrove, D. M., Gillinov, A. M. (1998). Partial Sternotomy for Mitral Valve Operations. Operative Techniques in Cardiac and Thoracic Surgery, 3(1), 62–72. doi:10.1016/s1085-5637(07)70007-4

[19] Pektok, E., Sierra, J., Cikirikcioglu, M., Müller, H., Myers, P. O., Kalangos, A. (2010). Midterm Results of Valve Repair With a Biodegradable Annuloplasty Ring for Acute Endocarditis. The Annals of Thoracic Surgery, 89(4), 1180–1185. doi:10.1016/j.athoracsur.2010.01.

[20] Devereux RB, Brown WT, Kramer-Fox R, Sachs I. Inheritance of mitral valve prolapse: effect of age and sex on gene expression. Ann Intern Med. 1982 Dec;97(6):826-32. doi: 10.7326/0003-4819-97-6-826. PMID: 7149490.

[21] Lilyasari, O., Prakoso, R., Kurniawati, Y., Roebiono, P. S., Rahajoe, A. U., Sakidjan, I., Harimurti, G. M. (2020). Clinical Profile and Management of Rheumatic Heart Disease in Children and Young Adults at a Tertiary Cardiac Center in Indonesia. Frontiers in Surgery, 7. doi:10.3389/fsurg.2020.00047

[22] Carpentier, A. F., Lessana, A., Relland, J. Y. M., Belli, E., Mihaileanu, S., Berrebi, A. J., ... Loulmet, D. F. (1995). The "Physio-Ring": an advanced concept in mitral valve annuloplasty. The Annals of Thoracic Surgery, 60(5), 1177–1186. doi:10.1016/0003-4975(95)00753-8

[23] Jorge-Herrero E, Fonseca C, Barge AP, Turnay J, Olmo N, Fernández P, Lizarbe MA, García Páez JM. Biocompatibility and calcification of bovine pericardium employed for the construction of cardiac bioprostheses treated with different chemical crosslink methods. Artif Organs. 2010 May;34(5):E168-76. doi: 10.1111/j.1525-1594.2009.00978.x. PMID: 20633147.

[24] Richardt, D., Bucsky, B., Charitos, E. I., Sievers, H. H., & Scharfschwerdt, M. (2014). A novel rigid annuloplasty ring for aortic valve reconstruction: an in vitro investigation. The Annals of thoracic surgery, 97(3), 811-815.

[25] Yakacki, C. M., Shandas, R., Safranski, D., Ortega, A. M., Sassaman, K., Gall, K. (2008). Strong, Tailored, Biocompatible Shape-Memory Polymer Networks. Advanced functional materials, 18(16), 2428–2435. https://doi.org/10.1002/adfm.200701049

[26] Zhang, L., Shang, L., & Gao, Y. (2019). Analytical Solutions of Functionally Graded Curved Beams under an Arbitrarily Directed Single Force. Mathematical Problems in Engineering, 2019.

7 Appendix

7.1 Stress Profile of Initially Curved Beams

From Zhang et. al. [26], the Airy's stress function for an initially curved beam, as in the case for our annuloplasty rings, is

$$\phi = \frac{mg}{rt}\sin\theta$$

which is related to the radial stress via,

$$\sigma(r,\theta) = \frac{1}{r}\frac{\partial\phi}{\partial r} + \frac{1}{r^2}\frac{\partial^2\phi}{\partial\theta^2}$$

Hence,

$$\sigma(r,\theta) = \frac{2mg\sin\theta}{r^3 t}$$

Note that stress is a function of r and θ. Hence, the averaged radial stress σ_r is obtained via,

$$\sigma_r = \frac{2}{\pi t}\int_0^{\frac{\pi}{2}}\int_{R-t}^{R}\frac{2mg\sin\theta}{r^3 t}\,dr\,d\theta = \frac{4mg}{\pi t^2}\left(\frac{1}{2(R-t)^2} - \frac{1}{2R^2}\right)$$

7.2 Moment of Inertia

The Nitinol and Physio rings have a circular cross-section, hence the Moment of Inertia is given by,

$$\begin{aligned} I = {} & \frac{R^2+(R-z)^2}{2}\left(\rho\pi w z\left(R-\frac{t}{2}\right)\right) + \frac{2\rho w t R(2R)^2}{12} \\ & + \left(\rho w t\left(\pi\left(R-\frac{t}{2}\right)+2R\right)\right)\left(R-\frac{t}{2}\right)^2 \end{aligned}$$

In contrast, the rectangular MMA-PEDGMA, with a width w, have the MOI

$$\begin{aligned} I = {} & \frac{R^2+(R-z)^2}{2}\left(\rho\pi^2\left(\frac{z}{2}\right)^2\left(R-\frac{t}{2}\right)\right) + \frac{2\rho\pi\left(\frac{z}{2}\right)^2 R(2R)^2}{12} \\ & + \left(\rho\pi\left(\frac{z}{2}\right)^2\left(\pi\left(R-\frac{t}{2}\right)+2R\right)\right)\left(R-\frac{t}{2}\right)^2 \end{aligned}$$

7.3 Percentage Reduction in Incision Size

The data collected for the Nitinol rings are presented in the table below:

Ring Thickness	Initial Cross-Section	Final Cross-Section	Percentage Reduction
0.25 mm	20.6 mm	8.23 mm	60.0%
0.50 mm	16.1 mm	7.75 mm	51.9%
1.00 mm	14.3 mm	12.6 mm	11.9%

The data collected for the MMA-PEGDMA rings are presented below:

Ring Thickness	Initial Cross-Section	Final Cross-Section	Percentage Ratio
1.00 mm	17.6 mm	1.00 mm	94.3%
2.00 mm	18.9 mm	5.80 mm	69.2%
3.00 mm	22.4 mm	7.26 mm	67.5%
4.00 mm	23.4 mm	10.4 mm	55.8%
5.00 mm	25.9 mm	10.8 mm	58.2%
6.00 mm	25.9 mm	14.7 mm	43.4%